EPJ Web of Conferences **182**, 02052 (2018) https://doi.org/10.1051/epjconf/201818202052
ICNFP 2017

$t\bar{t}H$ Coupling Measurement with the ATLAS Detector at the LHC

Asma HADEF, on behalf of the ATLAS Collaboration[1,a]

[1] *Centre de Physique des Particules de Marseille, Aix Marseille Univ, CNRS/IN2P3, CPPM, Marseille, France*

Abstract. The Higgs boson was discovered on the 4th of July 2012 with a mass around 125 GeV by ATLAS and CMS experiments at LHC. Determining the Higgs properties (production and decay modes, couplings,...) is an important part of the high-energy physics programme in this decade. A search for the Higgs boson production in association with a top quark pair ($t\bar{t}H$) at ATLAS [1] is summarized in this paper at an unexplored center-of-mass energy of 13 TeV, which could allow a first direct measurement of the top quark Yukawa coupling and could reveal new physics. The $t\bar{t}H$ analysis in ATLAS is divided into 3 channels according to the Higgs decay modes: $H \rightarrow$ Hadrons, $H \rightarrow$ Leptons and $H \rightarrow$ Photons. The best-fit value of the ratio of observed and Standard Model cross sections of $t\bar{t}H$ production process, using 2015-2016 data and combining all $t\bar{t}H$ final states, is 1.8 ± 0.7, corresponds to 2.8σ (1.8σ) observed (expected) significance.

1 Introduction

The Higgs boson production in association with a top quark pair $t\bar{t}H$ (Figure 1a) represents 1% of the total Higgs production making the observation of $t\bar{t}H$ very challenging with limited available statistics in Run 1. However, the expected SM $t\bar{t}H$ cross section increases by a factor of 3.9 from centre of mass energy of 8 TeV to 13 TeV. This factor, comparable to the one for the dominant backgrounds, allows to accumulate signal events at a faster rate at 13 TeV than during Run 1. Current efforts are dedicated to observe the $t\bar{t}H$ at the end of Run 2 with the full available statistics. The observation of the $t\bar{t}H$ production mode allows a direct measurement of the top Yukawa coupling (referred as $g_{t\bar{t}H}$): the strongest coupling to the Higgs boson, giving that the top quark is the heaviest fundamental particle in the SM, with a mass equal to 173.21 GeV [2]. Its measurement is estimated using the ggF production (Figure 1b) where the Higgs is indirectly coupled to the top quark via a loop but no new physics is assumed. Its value is found to be compatible with the SM expectation, using the top coupling modifier (κ_t : defined as the ratio between the observed and SM top quark yukawa coupling) estimated as 0.87 ± 0.15, combining ATLAS and CMS data at Run 1 [3]. However, new physics could be hidden in the loops mediating the Higgs production via ggF. This issue could be solved by performing the measurements in $t\bar{t}H$ production mode involving a direct, tree-level, Higgs-top coupling. Therefore, a search for $t\bar{t}H$ is used to allow a first direct measurement of the top quark Yukawa coupling that could reveal new physics. It is worth to mention that all results, discussed in this paper, are obtained from Refs [4–8].

[a] e-mail: asma.hadef@cern.ch

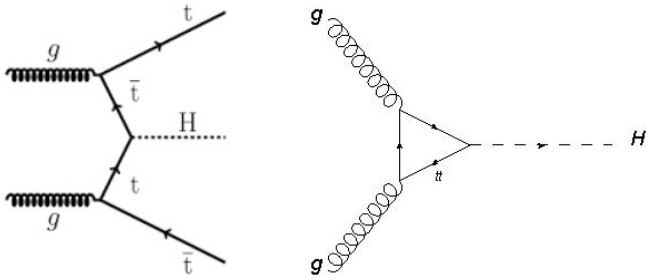

(a) $t\bar{t}H$ (b) ggF

Figure 1: Feynman diagram of (a) $t\bar{t}H$ and (b) ggF processes. The cross section of $t\bar{t}H$ is $\sigma_{t\bar{t}H} = 507$ fb at 13 TeV. The $t\bar{t}H$ process is tow order of magnitude lower than ggF: $\sigma_{t\bar{t}H}/\sigma_{ggF} \sim 0.01$.

2 Searches for $t\bar{t}H$ at ATLAS

A combination of searches for $t\bar{t}H$ production at 13 TeV has been performed by the ATLAS experiment in 3 Higgs decay channels: the $b\bar{b}$, multilepton using 13.2 fb^{-1} of luminosity [4, 7] and $\gamma\gamma$ using all available 2015/2016 data with luminosity of 36.1 fb^{-1} [5, 8]. To increase the sensitivity, each channel is categorised into sub-channels according to the number of leptons and hadrons. Every channel is discussed individually starting with $t\bar{t}H$ ($b\bar{b}$) representing the largest branching fraction.

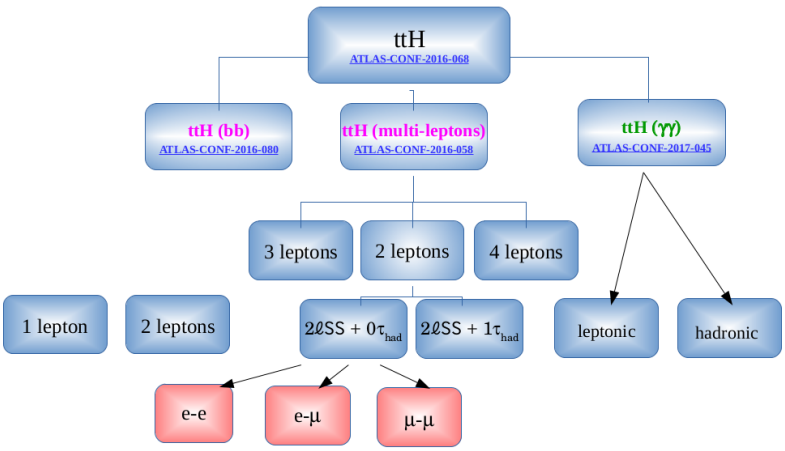

Figure 2: $t\bar{t}H$ analysis strategy in ATLAS experiment at 13 TeV with 13.2 fb^{-1} pp collision data.

Higgs decay modes	BR(%)
$H \to b\bar{b}$	58.1
$H \to WW$	21.5
$H \to \tau\tau$	6.3
$H \to ZZ$	2.8
$H \to \gamma\gamma$	0.2

Table 1: Branching ratios (BR) of the Higgs boson decay modes.

3 $t\bar{t}H$ ($b\bar{b}$) Analysis

3.1 Signal Region Selection

The signal region (SR) in this channel is divided into single- and di-lepton sub-channels. In single-lepton channel, exactly one lepton with at least 4 jets and at least 2 b-jets are required. In di-lepton channel, exactly 2 opposite sign (OS) leptons are required with at least 3 jets and 2 b-jets. The all hadronic channel is not treated yet at $\sqrt{s} = 13$ TeV. Events are further categorised according to the number of jets and b-jets as illustrated in the scheme of Figure 3a where each row corresponds to a different jet-multiplicity and each column represents a different b-jet-multiplicity in the single-lepton channel. Control regions (CR), sheded in blue, are used to constraint the uncertainties.

3.2 Background Estimation

The background in $t\bar{t}H$ ($b\bar{b}$) is dominating by $t\bar{t}$ +jets process ; divided according to the jet flavour into: $t\bar{t}$ +bjets, $t\bar{t}$ +c-jets and $t\bar{t}$ +light-jets. The pie-chart of Figure 3b shows the fractional contributions of the various backgrounds to the total background prediction in each region. The main background in the SR is $t\bar{t}$ +$b\bar{b}$. Followed by small contribution of non-$t\bar{t}$ background: single top, diboson W/Z+jets and fake leptons. The $t\bar{t}$ Background is estimated from simulation and normalised to the prediction before the fit. The normalization of $t\bar{t}$ +$b(c)$-jets background are free parameters of the fit. Finally, fake lepton background in the single lepton channels is estimated using data-driven method.

3.3 Signal/Background Separation

In order to separate the signal from the background, two stage Multivariate techniques are used. First, reconstruction BDT (shown by blue in the left plot of Figure 4) is trained to match the reconstructed jets to the partons emitted from top and Higgs decays in $t\bar{t}H$ simulation (shown by red). For this 26 input variables are considered in single lepton channels, chosen to achieve optimal performance. Then, for each SR, information from the output of the reco BDTs is combined with other kinematic variables in a classification BDT (shown in the right plot of Figure 4) with 21 input variables for single lepton channels.

3.4 Results

The post-fit yields of signal and total background are compared to data where the signal is normalised to the best fit value and to the excluded value. A good agreement is seen between data and expectation in all bins within the uncertainties. The best fit value of the signal strength measurements (μ) of the signal lepton channel, obtained from a profile likelihood fit, is 1.6 ± 1.1 where systematic uncertainties are dominating. The combination results have been removed because a problem was found in the di-lepton channel.

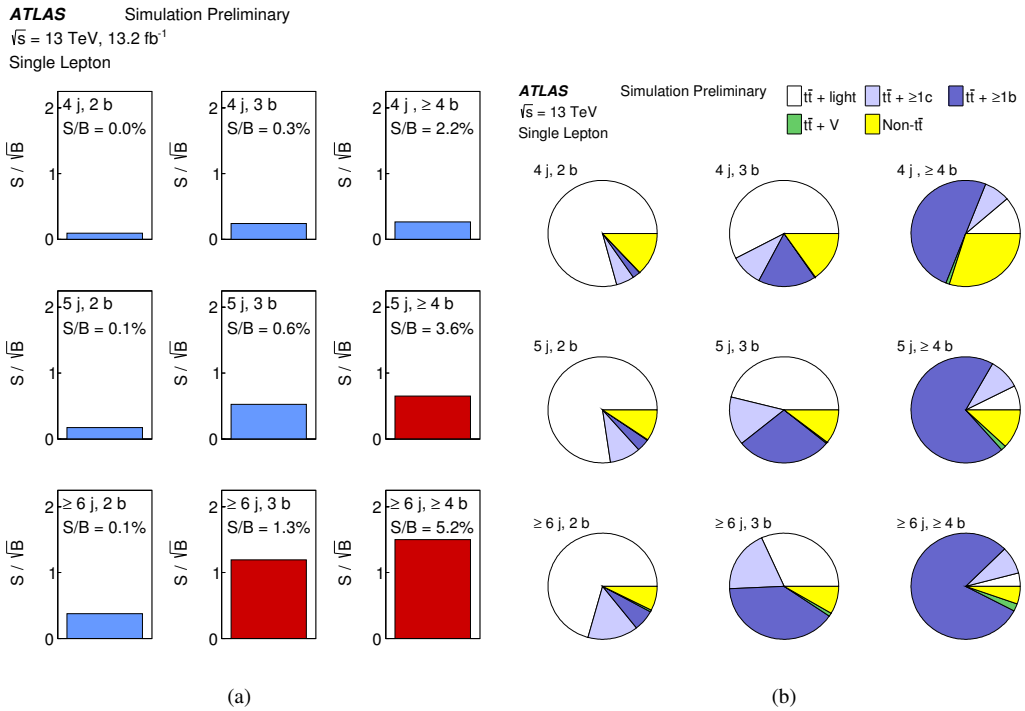

(a) (b)

Figure 3: (a) Single region (red) and control region (blue) definitions and (b) fractional contribution of the various background prediction in $t\bar{t}H$ ($b\bar{b}$) analysis for the single lepton channel in terms of b-jet and jet multiplicities [9].

4 $t\bar{t}H$ ($Multi-Lepton$) Analysis

4.1 Signal Region Selection

Events are categorised into six signal regions according to the number of light and hadronic tau leptons: 2ℓss (ee, $\mu\mu$ and $e\mu$), 2ℓss+$1\tau_{\text{had}}$, 3ℓ and 4ℓ. Three main decays are contributing: WW^*, $\tau\tau$ and ZZ^* as shown in Table 2a. The Higgs decay into two W bosons is the dominant decay for all sub-categories except for 2ℓss+$1\tau_{\text{had}}$ where Higgs decay into two tau leptons is dominating. The ZZ^* contribution is mostly $\ell\ell\nu\nu$ and $\ell\ell jj$ (since $H \rightarrow 4\ell$ is explicitly excluded in this analysis). The number of jets and b-jets differ from category to another and is summarized in Table 2b.

4.2 Background Estimation

Background is split into reducible and irreducible background as shown in Figure 5a. The reducible background is split into fake leptons (non-prompt leptons) and charge flip backgrounds. Fake leptons are coming from either mis-reconstructed objects as leptons, photon conversion or non prompt leptons decaying from heavy flavour jets. The latter is dominating in SRs. The charge flip background is mainly coming from the charge mis-reconstruction of an electron from bremsstrahlung. Reducible background is estimated using data-driven methods: the charge flip estimated from Z+jets OS events

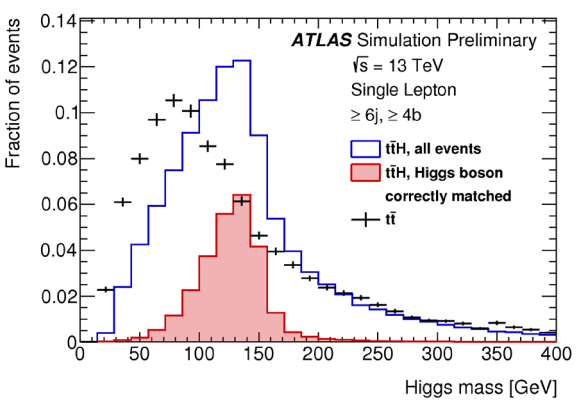

(a) BDT reco

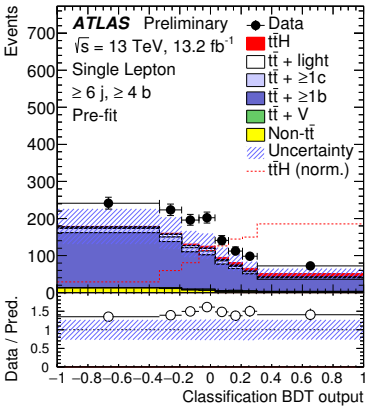

(b) BDT classification

Figure 4: BDT reconstruction and classification in $t\bar{t}H$ ($b\bar{b}$) analysis in Single lepton channel with at least 6 jets and 4 b-jets category [9].

Category	WW^*	$\tau\tau$	ZZ^*	Other
2ℓss	77 %	17 %	3 %	3 %
2ℓss+$1\tau_{\text{had}}$	46 %	51 %	2 %	1 %
3ℓ	74 %	20 %	4 %	2 %
4ℓ	72 %	18 %	9 %	2 %

(a)

SR	2ℓss	2ℓss+$1\tau_{\text{had}}$	3ℓ	4ℓ
Light Leptons	2SS	2 SS	3	4
Jets	≥ 5	≥ 4	$\geq 3\|\|4$	≥ 2
b-jets	≥ 1	≥ 1	$\geq 1\|\|2$	≥ 1
τ_{had}	0	1	-	-

(b)

Table 2: (a) Higgs boson decay modes and (b) Signal region definition in $t\bar{t}H$ (ML) analysis.

control region and fake leptons estimated from $t\bar{t}$ SS/OS events CRs. Prompt lepton background is estimated from simulation validated using four regions. Fake leptons are the dominant background in 2ℓss and 3ℓ channels as shown in Figure 5b.

4.3 Results

The pre-fit yields of signal and total background for each category in $t\bar{t}H$ (ML) is presented in Figure 6a. The best fit value of the signal strength $\mu_{t\bar{t}H}$ for each category and for the $t\bar{t}H$ (ML) combination is presented in Figure 6b. Systematic uncertainties on combination are dominating and listed in Figure 7. Fake leptons are driving the error on the total background estimated in the 2ℓss and 3ℓ channels. Observed (expected) 95% C.L. upper limit on $\mu_{t\bar{t}H}$ is 4.9 (2.3).

5 $t\bar{t}H$ ($\gamma\gamma$) Analysis

5.1 Signal Region Selection

The $t\bar{t}H$ ($\gamma\gamma$) channel has excellent di-photon mass resolution which is also sensitive to the tH channel (σ_{tH} = 74 fb). Event are categorised according to the number of leptons and tH/$t\bar{t}H$ channels: three

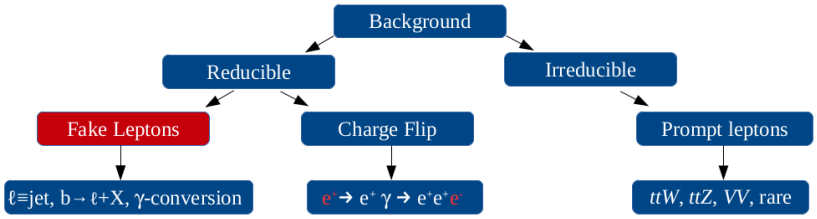

(a)

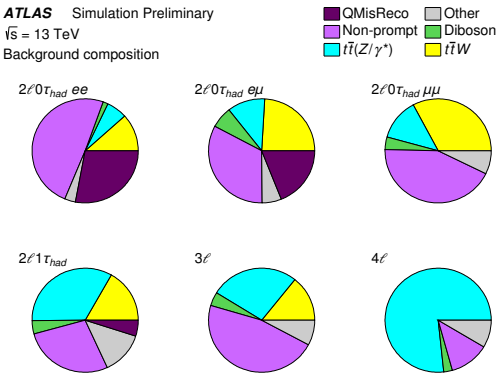

(b)

Figure 5: (a) Background estimation strategy and (b) fractional contribution of the various background prediction in $t\bar{t}H$ (ML) analysis [4].

leptonic channels, two of them are tH channels and six hadronic channels, 2 of them are tH channels. Cut&Count analysis is used in every category except the hadronic $t\bar{t}H$ channels where a BDT analysis is instead used. The number of jets and b-jets requirements for leptonic and hadronic channels are shown in Table 3. The signal is modeled using a double-sided Crystal Ball function where its parameters are fitted to the simulated signal samples.

SR	Leptonic	Hadronic
Leptons	≥ 1	0
Jets	multiple	≥ 3
b-jets	≥ 1 central	≥ 1

Table 3: Signal region definition in $t\bar{t}H$ ($\gamma\gamma$) analysis.

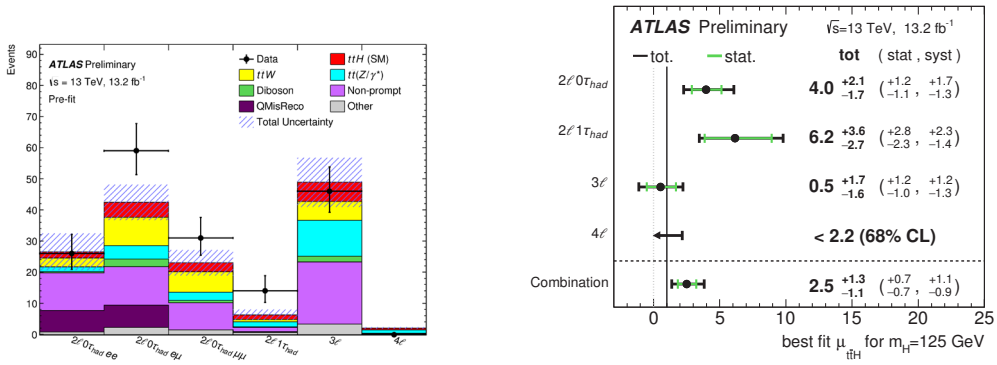

(a) (b)

Figure 6: (a) The pre-fit yields of signal and total background and (b) the best fit value of the signal strength in $t\bar{t}H$ (ML) analysis [4].

Uncertainty Source	$\Delta\mu$	
Non-prompt leptons and charge misreconstruction	$+0.56$	-0.64
Jet-vertex association, pileup modeling	$+0.48$	-0.36
$t\bar{t}W$ modeling	$+0.29$	-0.31
$t\bar{t}H$ modeling	$+0.31$	-0.15
Jet energy scale and resolution	$+0.22$	-0.18
$t\bar{t}Z$ modeling	$+0.19$	-0.19
Luminosity	$+0.19$	-0.15
Diboson modeling	$+0.15$	-0.14
Jet flavor tagging	$+0.15$	-0.12
Light lepton (e,μ) and $\tau_{\rm had}$ ID, isolation, trigger	$+0.12$	-0.10
Other background modeling	$+0.11$	-0.11
Total systematic uncertainty	$+1.1$	-0.9

Figure 7: Main Systematic sources in $t\bar{t}H$ (ML) analysis [4].

5.2 Background Estimation

A data driven method is used to estimate the continuum background coming from $\gamma\gamma$+jets, γ+jets and multi-jets. The shape of the background is build by reverting the photon identification or isolation criteria or removing b-tagging requirement. The shape is then normalised to data in the $m_{\gamma\gamma}$ distribution outside the $120 < m_{\gamma\gamma} < 130$ region. $\gamma\gamma$ and Vγ backgrounds are estimated from simulation. The total background with the fitted signal agree well with the expectation as shown in Figure 8.

5.3 Results

The best fit value of the signal strength $\mu_{t\bar{t}H}$ for $t\bar{t}H$ ($\gamma\gamma$) analysis is obtained from a $\tau_{maximum}$ likelihood fit for each event category and shown in the top of Figure 9. It corresponds to 1σ observed significance. Statistical uncertainties are dominating. Observed (expected) 95% C.L. upper limit on $\mu_{t\bar{t}H}$ are 1.7 (2.3).

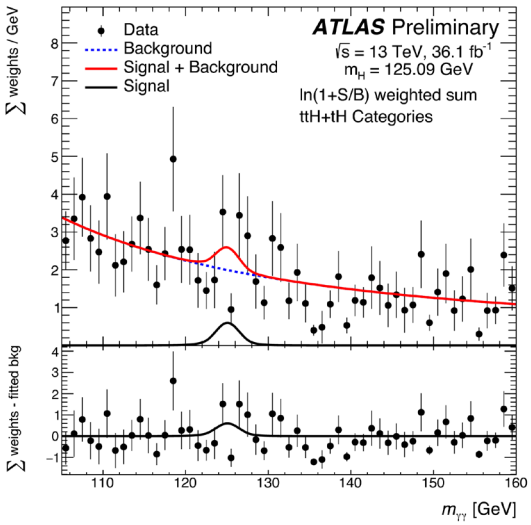

Figure 8: Di-photon invariant mass distribution in $t\bar{t}H$ ($\gamma\gamma$) analysis [5].

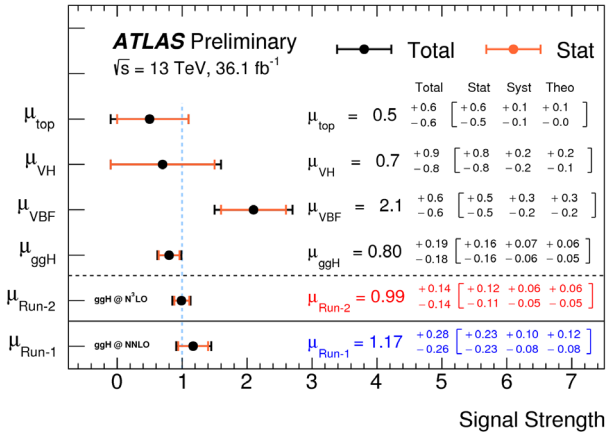

Figure 9: The best fit value of the signal strength in $t\bar{t}H$ ($\gamma\gamma$) analysis [5].

6 $t\bar{t}H$ ($ZZ^* \to 4\ell$) Analysis

As mentioned in Section 4, the $t\bar{t}H$ ($ZZ^* \to 4\ell$) channel is treated separately. A brief description of this analysis is presented in the following using 36.1 fb^{-1} of pp collision data at $\sqrt{s}$ =13 TeV. Despite the branching ratio of the Higgs decay to $ZZ^* \to 4\ell$ is only 0.01%, this channel is privileged thanks to its clear signature and the high Signal/Background ratio. A quadruplet leptons originating from a Higgs boson decay are selected, shown by blue histogram in Figure 10a which is well separated from the resonant $ZZ^* \to 4\ell$ background shown by the peak of the red histogram. The signal regions are classified according to the lepton flavour into 4 categories: $4e, 2e2\mu, 2\mu2e$ and 4μ. At least one b-jet

is required with either at least four additional jets or one additional lepton with $p_T > 15$ GeV and at least two jets. The main background in the analysis is the non resonant ZZ^*, shown by the tail of the red histogram in Figure 10a. Other background could also contribute coming from triboson, $t\bar{t}+Z$, $t\bar{t}$, Z+jets and WZ. Due to the limited number of events in the control regions, the signal strength is just limited to be less than 7.5 (Figure 10b) where the fit parameters are constrained to positive values to avoid instabilities in the fit configuration.

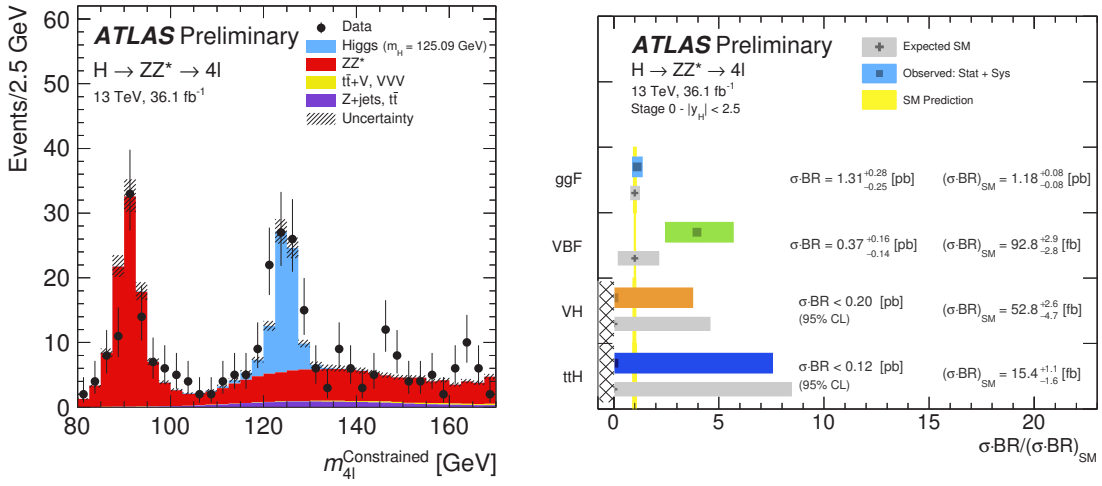

(a) (b)

Figure 10: (a) The quadruplet leptons invariant mass distribution and (b) the best fit value of the signal strength in $t\bar{t}H$ ($ZZ^* \to 4\ell$) analysis [6].

7 $t\bar{t}H$ Combination

There are two combination done at Run 2 so far: with 13.2 fb^{-1} data collision using $t\bar{t}H$ ($b\bar{b}$), (ML) and ($\gamma\gamma$) channels [7] and with 36.1 fb^{-1} data collision using both $t\bar{t}H$ and tH channels with only $\gamma\gamma$ and $ZZ^* \to 4\ell$ Higgs decays [8]. The best fit value of the signal strength for 13.2 fb^{-1} data is 1.8 ± 0.7 which corresponds to 2.8σ observed significance. The observed (expected) 95% C.L upper limit on $\mu_{t\bar{t}H}$ is found to be 3.0 (1.2). The 13.2 fb^{-1} combination has smaller uncertainty than Run 1. Concerning the 36.1 fb^{-1} combination, 10% to 60% uncertainty reduction is achieved with respect to Run 1 $t\bar{t}H$ ($\gamma\gamma$) analysis. The ration of the cross sections between the $t\bar{t}H$ and ggF is also computed and found to be $0.007^{+0.010}_{-0.009}$. The ratio between the top and gluon modifiers (called λ_{tg}) is also computed and found to be $0.74^{+0.41}_{-0.63}$. In total, all combined results are found to be consistent with the SM prediction.

8 Conclusion

Searches for the $t\bar{t}H$ production are performed in the $t\bar{t}H$ ($b\bar{b}$), $t\bar{t}H$ (multileptons) and $t\bar{t}H$ ($\gamma\gamma$) channels using 13.2 fb^{-1} of pp collision data at 13 TeV recorded by the ATLAS experiment. Results with

full 2015-2016 data (36.1 fb^{-1}) are obtained for $t\bar{t}H$ ($\gamma\gamma$) and $t\bar{t}H$ ($ZZ^* \to 4\ell$) only combining $t\bar{t}H$ and tH production modes. Overall, consistency with the Standard Model expectation is observed.

References

[1] ATLAS collaboration, The ATLAS Experiment at the CERN Large Hadron Collider, 2008 JINST 3 S08003

[2] Particle Data Group, Review of Particle Physics, Chin. Phys. **C40**, 100001 (2016)

[3] ATLAS and CMS collaboration, Measurements of the Higgs boson production and decay rates and constraints on its couplings from a combined ATLAS and CMS analysis of the LHC pp collision data at $\sqrt{s}$ = 7 and 8 TeV, arXiv:1606.02266 [hep-ex], https://arxiv.org/abs/1606.02266

[4] ATLAS collaboration, Search for the Associated Production of a Higgs Boson and a Top Quark Pair in Multilepton Final States with the ATLAS Detector, ATLAS-CONF-2016-058, http://cds.cern.ch/record/2206153

[5] ATLAS collaboration, Measurements of Higgs boson properties in the diphoton decay channel with 36.1 fb^{-1} pp collision data at the center-of-mass energy of 13 TeV with the ATLAS detector, ATLAS-CONF-2017-045, http://cds.cern.ch/record/2273852

[6] ATLAS collaboration, Measurement of the Higgs boson coupling properties in the $H \to ZZ^* \to 4\ell$ decay channel at $\sqrt{s}$ = 13 TeV with the ATLAS detector, ATLAS-CONF-2017-043, http://cds.cern.ch/record/2273849

[7] ATLAS collaboration, Combination of the searches for Higgs boson production in association with top quarks in the $\gamma\gamma$, multilepton, and $b\bar{b}$ decay channels at $\sqrt{s}$=13 TeV with the ATLAS Detector, ATLAS-CONF-2016-068, http://cds.cern.ch/record/2206211

[8] ATLAS collaboration, Combined measurements of Higgs boson production and decay in the $H \to ZZ^* \to 4\ell$ and $H \to \gamma\gamma$ channels using $\sqrt{s}$ = 13 TeV pp collision data collected with the ATLAS experiment, ATLAS-CONF-2017-047, https://cds.cern.ch/record/2273854

[9] ATLAS collaboration, Search for the Standard Model Higgs boson produced in association with top quarks and decaying into $b\bar{b}$ in pp collisions at $\sqrt{s}$ = 13 TeV with the ATLAS detector, ATLAS-CONF-2016-080, http://inspirehep.net/record/1480060/files/ATLAS-CONF-2016-080.pdf